

Equilibrium orientations of diatomic-molecular impurities in cubic crystals determined by a polarized Raman study of the stretching mode

Hilde Fleurent, Wim Joosen, and Dirk Schoemaker

Physics Department, University of Antwerp (Universitaire Instelling Antwerpen), B-2610 Antwerpen (Wilrijk), Belgium

(Received 8 March 1988)

Polarized Raman measurements were performed on the A_1 stretching mode of static or reorienting diatomic molecular impurities in cubic crystals. The equilibrium orientation(s) of the molecular axes, most commonly lying along either the $\langle 110 \rangle$, $\langle 111 \rangle$, or $\langle 100 \rangle$ directions, can be determined by a behavior-type (BT) analysis of the Raman spectra. This approach allows one to establish the point group of the impurity ion without (i) applying any secondary fields or (ii) studying the experimentally less accessible tunneling sidebands. The correspondence between the polarized Raman intensities and the actual defect symmetry can be obscured when the stretching vibration is strongly coupled to reorientational degrees of freedom, or, when the anisotropy of its derived polarizability is relatively small. The BT analysis was tested on the stretching modes of CN^- in KCl and KBr, OD^- in KCl, and O_2^- in KCl and KBr, establishing a C_{3v} , C_{4v} , and D_{2h} point-group symmetry, respectively. The C_{4v} symmetry for OH^- in KCl and KBr is confirmed and a lower symmetry for OH^- in NaCl is established. The SH^- defect in KCl is shown to possess C_{3v} symmetry. A comparison is made between the present Raman results and previous experimental work.

I. INTRODUCTION

Reorienting substitutional molecular defects in alkali halides have been studied thoroughly over the years. In order to describe their reorientational motion at low temperatures two different models have been developed: (i) The Devonshire model¹ studies the energy levels of a classical free rotor perturbed by a cubic crystal field and establishes potential minima along $\langle 100 \rangle$, $\langle 111 \rangle$, and $\langle 110 \rangle$. (ii) More recently, theoretical models were presented of quantum mechanical tunneling of defects in a cubic multiwell potential.^{2,3} The simplest tunneling models describe directional states with C_{4v} , C_{3v} , and C_{2v} point-group symmetry (D_{4h} , D_{3d} , and D_{2h}) for heteronuclear (homonuclear) molecular ions. Narayanamurti and Pohl⁴ and, more recently, Bridges⁵ have published extensive reviews of the theoretical and experimental contributions on this matter.

Several experimental techniques studied the behavior of the defect under stress or electric fields and allowed one to deduce the symmetry of the multiwell potential for OH^- , OD^- , CN^- , and O_2^- in alkali halides. In contrast, Raman scattering has been used to probe the dynamical properties of (reorienting) defects once the symmetry was investigated.⁶⁻¹⁰ Durand and Lüty were the first to determine the symmetry of the potential wells through a Raman study of the tunneling sidebands of the CN^- defect in KCl.¹¹

In the present paper it will be shown that the behavior-type (BT) analysis of the polarized Raman spectra of the high-frequency stretching mode is a straightforward method to establish the equilibrium orientations of reorienting diatomic molecular defects without field-induced molecular alignment.

The BT method^{12,13} was first applied to study the local modes of the foreign halogen (Y^-) perturbed H^0 center [$\text{H}^0(Y^-)$] in different alkali halides¹⁴ and the Li^+ -perturbed H^0 center [$\text{H}^0(\text{Li}^+)$] in KCl.¹⁵ Subsequently, the BT method was used to interpret the resonant Raman spectra of $\text{TI}^0(1)$ in several alkali halides,^{16,17} and of $\text{In}^0(1)$ and $\text{Ga}^0(1)$ in KCl.¹⁸ An extension was necessary to analyze the polarized Raman spectra of the $F_A(\text{Li}^+)$ center in KCl and KBr,^{19,20} and of the TI^+ -unperturbed $\text{TI}^0(1)$ center in KCl, KBr, and RbCl.²¹ The investigation of the low-frequency resonance of the off-center Li^+ defect in KCl contributed to the understanding of its anomalous isotope shift observed upon ^6Li -to- ^7Li substitution.^{22,23}

The equilibrium orientations will be determined from the polarized Raman spectra of the *stretching* modes of OH^- , OD^- , CN^- , and O_2^- in several alkali halides. For these defect systems the symmetry was established earlier by several other experimental techniques. The molecular axes of OH^- in KCl, KBr, and NaCl lie along $\langle 100 \rangle$.²⁴⁻²⁹ The investigation of CN^- was hampered for some time by inaccurately interpreted experimental data,^{30,31} but finally, a $C_{3v}\langle 111 \rangle$ symmetry was established.^{11,32-34} Electron paramagnetic resonance (EPR) measurements on the O_2^- ion revealed its potential wells lying along $\langle 110 \rangle$.³⁵⁻³⁷ We also establish the C_{3v} symmetry for the SH^- center in KCl.³⁸

II. EXPERIMENTAL DETAILS

The CN^- vibration was studied in KCl and KBr crystals containing typically 0.5 wt. % of KCN added to the melt. KCl: OD^- was doped with 0.6 mol % OD^- . The KCl: SH^- samples were grown under a H_2S vapor pressure of 3 Torr. The measurements on O_2^- were per-

formed on KCl, KBr, and NaCl crystals containing about 1 mol % of the corresponding alkali-peroxyde. The Raman spectra were excited with an Ar⁺ laser (514.5 and 488.0 nm) and a Kr⁺ laser (530.9 nm) at temperatures between 8 and 14 K. Details about the Raman setup can be found in Ref. 12.

III. BEHAVIOR-TYPE METHOD

A. General idea

The BT method developed for the analysis of polarized Raman spectra of randomly or preferentially oriented defects in cubic crystals allows one to determine within clearly spelled-out limits the defect symmetry and the irreducible representation of the studied vibrational mode.

The symmetry related form of the second-rank Raman tensor is known from group theory³⁹. The observed polarized Raman scattering intensity is obtained by a discrete average over all the equivalent orientations of the molecular defect. The BT method shows that the information about the defect symmetry, contained in the Raman tensor, is not completely washed out by this space average, such that the symmetry of the directional states of the molecular axis can be distinguished (see Sec. III C).

The essential point of the method¹² is the characterization of an observed dynamical mode by a set of independent intensity parameters (IP) deducible from the polarized Raman spectra obtained in the traditional perpendicular scattering geometry. The IP's are interrelated by some simple arithmetical expressions, depending on the Raman tensor of the mode and on the defect distribution among its possible orientations. These relations, which have been listed in Ref. 12, define the behavior type (BT) of the mode. The following limitations are intrinsic to the BT method:¹² (i) Only 25 *representative* dynamical modes can be distinguished, and (ii) the observed BT may exhibit a higher symmetry than the actual BT. This case is called "accidental degeneracy" throughout this paper.

B. Behavior-type method for randomly oriented defects

In the BT method the measured Raman intensities are expressed in terms of the IP. For randomly oriented defects in cubic crystals, three independent IP's called s , r , and q can be determined. These IP are functions of the components of the second rank Raman tensor T :

$$s = 8kNI_0(T_{12}^2 + T_{13}^2 + T_{23}^2), \quad (1a)$$

$$r = 8kNI_0(T_{11}T_{22} + T_{11}T_{33} + T_{22}T_{33}), \quad (1b)$$

$$q = 8kNI_0(T_{11}^2 + T_{22}^2 + T_{33}^2), \quad (1c)$$

in which k is an instrumental efficiency factor, I_0 is the intensity of the exciting light beam, and N is proportional to the defect concentration.

The ratios s/q and r/q characterize the defect symmetry and the irreducible representation of its vibrational modes. For randomly oriented defects, seven different sets of IP relations, i.e., seven different BT's can be distinguished (Table VIII in Ref. 12). The observed BT corresponds to a set of possible dynamical modes and defect

symmetries (Table VI in Ref. 12). The polarized Raman intensities are designated by $I_{\alpha\beta}$ in which α and β represent the polarization directions of the incident and the detected scattered light, expressed in the reference frame of the crystal $\langle 100 \rangle$ directions. The Raman intensities equivalent to those of set 1 of optical geometry pairs (OGP) (Table XI in Ref. 12) yield the s/q ratio:

$$I_{xy} \equiv I_{xz} \equiv I_{yz} = s, \quad (2a)$$

$$I_{yy} = q, \quad (2b)$$

$$I_{y,yz} \equiv I_{y,yz} = \frac{1}{2}(s + q). \quad (2c)$$

From OGP set 3 one can determine the s/q and r/q values:

$$I_{xy,z} \equiv I_{x\bar{y},z} = s, \quad (3a)$$

$$I_{x\bar{y},x\bar{y}} = \frac{1}{2}(q + r) + s, \quad (3b)$$

$$I_{xy,x\bar{y}} = \frac{1}{2}(q - r). \quad (3c)$$

C. Behavior-type analysis of stretching vibrations of molecular defects

Nonresonant Raman scattering is an instantaneous process.⁴⁰ Consequently, the polarized Raman spectra of the stretching vibration reflect the low symmetry of the directional states along $\langle 110 \rangle$, $\langle 111 \rangle$, or $\langle 100 \rangle$, and not an averaged cubic symmetry resulting from the reorientational motion between these equivalent directional states.

The stretching mode of a *free* diatomic molecule belongs to the totally symmetric representation of $C_{\infty v}$. When expressed in the frame (x', y', z') with z' along the molecular axis, its Raman tensor has the following form:

$$C_{\infty v}(A_1): \begin{pmatrix} a & 0 & 0 \\ 0 & a & 0 \\ 0 & 0 & a_3 \end{pmatrix}. \quad (4)$$

In the cubic lattice the form of the Raman tensor of the stretching mode depends on the orientation of the molecular axis. For heteronuclear diatomic impurities oriented along $\langle 100 \rangle$, $\langle 111 \rangle$, and $\langle 110 \rangle$, the Raman tensors, expressed in the crystal reference frame with $x \parallel [100]$, $y \parallel [010]$, and $z \parallel [001]$ are the following:

$$C_{4v}(A_1): \begin{pmatrix} a & 0 & 0 \\ 0 & a & 0 \\ 0 & 0 & a_3 \end{pmatrix}, \quad (5a)$$

$$C_{3v}(A_1): \begin{pmatrix} a' & b' & b' \\ b' & a' & b' \\ b' & b' & a' \end{pmatrix}, \quad (5b)$$

$$C_{2v}(A_1): \begin{pmatrix} h' & -c' & 0 \\ -c' & h' & 0 \\ 0 & 0 & a_2 \end{pmatrix}. \quad (5c)$$

Following the notations of Ref. 12 the symbols used in (5) stand for

TABLE I. The four observed behavior types (BT's), which can possibly be derived for the *totally symmetric* mode of randomly oriented defects. The BT's are defined by the arithmetic relations between the q , r , and s intensity parameters (IP's) and are numbered according to Ref. 12. The actual symmetries for diatomic impurities are indicated.

BT number	q	s	r	Symmetries
13	q	0	q	
39	q	s	q	$C_{3v}[111], D_{3d}[111]$
50	q	0	r	$C_{4v}[100], D_{4h}[100]$
60	q	s	r	$C_{1h}(010), C_{1h}(110), C_{2v}[110], D_{2h}[110]$

$$a = \frac{1}{2}(x'x' + y'y'), \quad a_3 = z'z', \quad (6a)$$

$$a' = \frac{2}{3}a + \frac{1}{3}a_3, \quad b' = \frac{1}{3}(a_3 - a), \quad (6b)$$

$$h' = \frac{1}{2}(x'x' + z'z'), \quad c' = \frac{1}{2}(z'z' - x'x'), \quad a_2 = y'y'. \quad (6c)$$

It has to be noted that the expressions (6c) for the components of the Raman tensor (5c) have been corrected in comparison with Ref. 12. The Raman tensors (5) also apply to homonuclear molecular impurities.

Since we are studying the stretching vibration, i.e., a totally symmetric mode, the number of different BT's, which can be derived from the polarized Raman data, reduces from seven to four. These four BT are listed in Table I.

IV. EXPERIMENTAL RESULTS

A. Accuracy, sample orientation, and calculation of the s/q and r/q ratios

Table II contains the s/q and r/q values for several vibrational stretching modes. It illustrates the importance of very accurate polarized Raman measurements. Without a precise knowledge of the accuracy it is impossible to distinguish between an IP being zero (one) or being very close to zero (one). Therefore, we have very carefully tested the alignment of the laser beam and of the polarization directions on the polarized Raman properties of the totally symmetric mode of CCl_4 , (at 460 cm^{-1}) in the liquid phase. We have measured the intensities analogous to those of OGP set 1 [see (2)]. The breathing mode of CCl_4 is characterized by a zero s/q ratio,⁴¹ or equivalently, a zero depolarization ratio ρ .⁴² Moreover, the equality in (2c) should hold for any mode, when the experimental setup is accurately aligned. In our reference measurements on liquid CCl_4 we systematically achieved values for s/q and $I_{y,yz}/I_{y,y\bar{z}}$ of the 460-cm^{-1} mode, better than 0.008 and 0.99, respectively (see Fig. 1).

Misalignment of the crystal axes in the laboratory reference frame obscures the actual s/q and r/q ratios. In Table XIV of Ref. 12 the errors on the polarized Raman intensities are calculated as a function of small-angle rotations of the sample around the three crystal directions. It can be verified that improvement of the 45° setup, associated with the relation (2c), guarantees the s/q and r/q values well determined to second order in the deviation angles. However, the expansion for small devia-

tion angles is not valid when s/q is close to zero and r/q is close to unity. This is the case for the CN^- ion in KCl and KBr. For this center we have evaluated the errors by simultaneous measurements on CN^- and a "sensitive" defect, e.g., SH^- , and by testing the reproducibility of the values for CN^- .

Some representative spectra are shown in Figs. 1–3. A set of calibration measurements on liquid CCl_4 is included as a reference for the experimental accuracy.

Equations (2) and (3) permit the calculation of the s/q and r/q values from the polarized Raman data. The results are presented in Table II.

B. Analysis of the polarized Raman data

1. OH^-

Peascoe *et al.*^{8,9} presented the polarized Raman data for OH^- in KCl, KBr, and NaCl. The spectra are conventionally denoted as A_{1g} , T_{2g} , and E_g . Starting from the relations

$$I_{xy,z} = \frac{1}{2}T_{2g}, \quad (7a)$$

$$I_{xy,x\bar{y}} = \frac{3}{4}E_g, \quad (7b)$$

$$I_{xy,xy} = A_{1g} + \frac{1}{4}E_g + \frac{1}{2}T_{2g}, \quad (7c)$$

one can relate the A_{1g} , T_{2g} , and E_g spectra to the s/q and r/q values:

$$s = \frac{1}{2}T_{2g}, \quad (8a)$$

$$q = A_{1g} + E_g, \quad (8b)$$

$$r = A_{1g} - \frac{1}{2}E_g. \quad (8c)$$

The s/q and r/q ratios, which we derived from the spectra and the numerical results of Refs. 8 and 9, are presented in Table II. For OH^- in KCl and KBr, BT 50, corresponding to the C_{4v} symmetry, is established. The s/q value of 0.06 for $\text{NaCl}:\text{OH}^-$ can be interpreted either as being definitely different from zero, or as erroneously different from zero because of inaccurate alignment. We did not perform any measurements on OH^- , but we measured the s/q for $\text{KCl}:\text{OD}^-$. The obtained s/q ratio of 0.00 ± 0.01 , clearly pointing to BT 50, convinced us that accurate polarized Raman measurements do allow one to deduce unquestionably the zero character of a particular IP. Assuming that the measurements in Ref. 8 on OH^- in NaCl were performed with the same accuracy as those

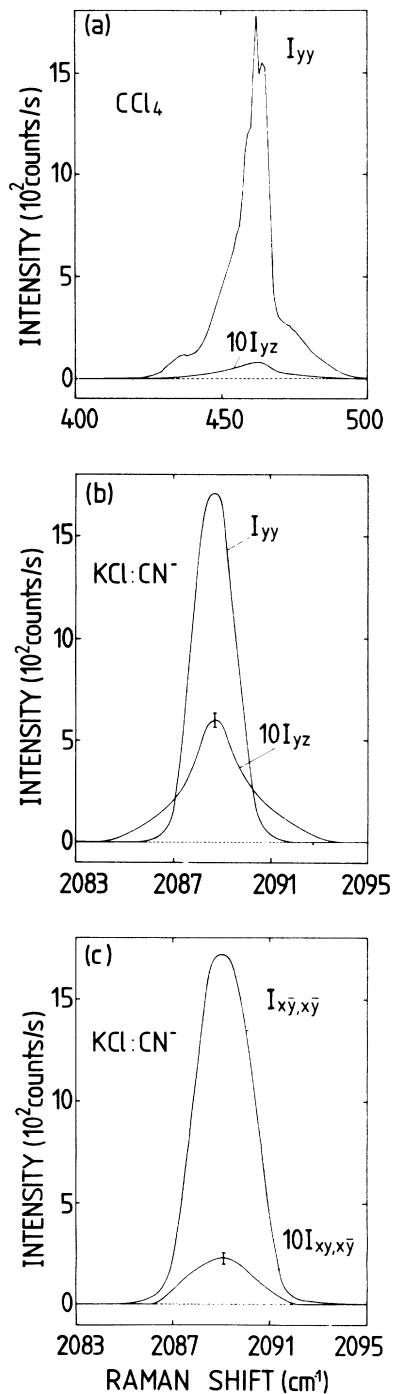


FIG. 1. Polarized Raman spectra of the totally symmetric mode of liquid CCl_4 (a) illustrating the attained experimental accuracy, and of the A_1 mode of CN^- in KCl measured in {100} cut samples (yielding s/q) (b), and in {110} polished samples (yielding s/q and r/q) (c). The broadening of the yz spectrum (b) reflects the sidebands (Sec. V). All spectra were excited at 530.9 nm (Kr^+ laser, 100 mW). A constant background, different for each spectrum, was subtracted for easier mutual comparing. The intensities in (a) and (b) were divided by 33 and 2.5, respectively. The spectra have been smoothed. Unless explicitly indicated by error bars, the statistical fluctuations are 10 counts/sec. The fine structure in (a) is due to different combinations of chlorine isotopes in CCl_4 .

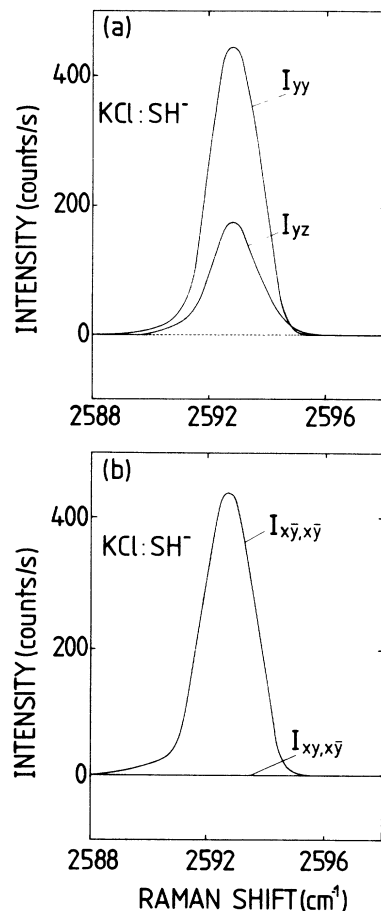


FIG. 2. Polarized Raman spectra of the A_1 mode of SH^- in KCl measured in a {100} cut sample (a), and in a {110} polished sample (b). The intensities in (b) have been divided by 2.5. The spectra were excited at 514.5 nm (Ar^+ laser, 350 mW). Constant backgrounds were subtracted. The statistical fluctuations are about 6 counts/sec.

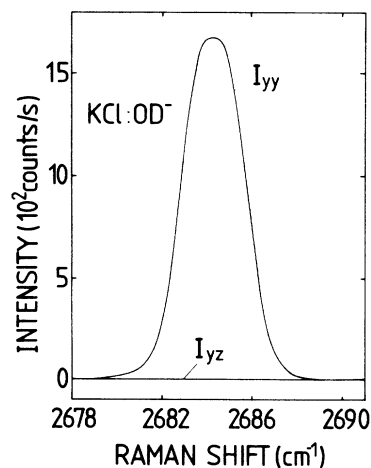


FIG. 3. Polarized Raman spectra of the A_1 mode of OD^- in KCl, measured in a {100} cut sample under 488.0 nm excitation (Ar^+ laser, 500 mW). The statistical fluctuations are about 10 counts/sec. The yz spectrum coincides with the baseline.

TABLE II. Results of the behavior-type (BT) analysis of the stretching mode for several diatomic molecular ions in different alkali halides. Peak positions are given together with the experimentally determined s/q and r/q ratios and the corresponding BT, according to Ref. 12. The observed BT symmetry is compared to the actual symmetry as determined by other experimental techniques. Note the "accidental degeneracy" for $\text{NaCl}:\text{O}_2^-$.

		Peak position (cm^{-1})	s/q	r/q	BT number	Observed BT symmetry	Actual symmetry
CN^-	KCl	2089	0.04 ± 0.01	0.98 ± 0.03	39	C_{3v}	C_{3v}^a
	KBr	2078	0.04 ± 0.01	0.98 ± 0.03	39	C_{3v}	C_{3v}^b
SH^-	KCl	2593	0.38 ± 0.03	0.97 ± 0.07	39	C_{3v}	C_{3v}^c
	KCl	1149	0.28 ± 0.04	0.39 ± 0.05	60	D_{2h}	D_{2h}^d
O_2^-	KBr	1137	0.26 ± 0.07	0.40 ± 0.12	60	D_{2h}	D_{2h}^d
	NaCl	1148	0.40 ± 0.07	0.95 ± 0.07	39	D_{3d}^e	D_{2h}^d
	KCl	3643	0.02	0.78	50	C_{4v}	C_{4v}^f
OH^{-g}	KBr	3618	0.01	0.75	50	C_{4v}	C_{4v}^h
	NaCl	3652	0.06	0.85	60	C_{1h}	C_{4v}^i, C_{1h}^j
OD^-	KCl	2685	0.00 ± 0.01		50	C_{4v}	

^aFrom Refs. 11, 32, 33, and 34.

^bFrom Ref. 33.

^cFrom Ref. 38.

^dFrom Refs. 35, 36, and 37.

^eCase of accidental degeneracy (see Sec. IV).

^fFrom Refs. 24, 26, 27, 28, and 29.

^gRaman data from Refs. 8 and 9: Errors are not estimated for these s/q and r/q ratios.

^hFrom Refs. 24, 26, and 28.

ⁱFrom Refs. 25, 27, and 28.

^jFrom Ref. 47.

in KCl and KBr,⁹ we consider the s/q ratio in $\text{NaCl}:\text{OH}^-$ as being different from zero. The consequences of this assumption are considered in Sec. V.

2. CN^-

We have interpreted the s/q value of 0.04 in both $\text{KCl}:\text{CN}^-$ and $\text{KBr}:\text{CN}^-$ as nonzero. The reproducibility of this ratio in six independent experiments and in crystals with different CN^- concentrations, together with the measurements on $\text{KCl}:\text{OD}^-$ (see Sec. IV B 1), support this interpretation. Consequently, the observed BT of CN^- in KCl and KBr corresponds to the C_{3v} point group. The s/q value of 0.04 originates from the relatively small anisotropy of the *derived* polarizability (See Sec. V).

For all investigated molecular impurities a comparison was made between the s/q and r/q ratios calculated with peak height intensities and integrated areas. Both ways gave identical results *except* for CN^- . The integrated intensities provide evidence for sidebands only in the T_{2g} spectrum as was established earlier by Durand and Lüty.¹¹

3. O_2^-

The polarized Raman spectra of O_2^- in KCl and KBr possess a BT 60, corresponding to the D_{2h} symmetry. The similarity of the data in KCl and KBr contrasts with the measurements on O_2^- in NaCl (Table II). Clearly, there is a strong influence from the surrounding ions. The r/q ratio, which is in NaCl very close to unity, reveals a BT 39, associated with a D_{3d} [111] symmetry. This is at variance with the EPR measurements on O_2^- ,³⁵⁻³⁷ establishing the D_{2h} symmetry in KCl, KBr, and NaCl. However, BT 39 is consistent with BT 60 (Table X in Ref. 12). This "accidental degeneracy" illustrates one of the major limitations of the BT method.

The large experimental errors, mainly statistical errors due to the relatively weak Raman signals of O_2^- in NaCl, make a distinction between the BT 60 and the BT 39 impossible. Smaller error bars on the r/q ratio could lift the accidental degeneracy. We note that the s/q value of 0.26 for O_2^- in KBr is in strong disagreement with the earlier reported 0.04 value.¹⁰

4. SH^-

For SH^- in KCl, BT 39 is established corresponding to the C_{3v} symmetry. This is in disagreement with results by Chi and Nixon⁴³ obtained with the infrared absorption technique: A "reasonably good fit" was found with the simple Devonshire model for equilibrium orientations along $\langle 100 \rangle$. Bron and Dreyfus⁴⁴ also interpreted their paraelectric resonance spectra in terms of a $\langle 100 \rangle$ orientation for the SH^- axis. Otto's infrared measurements,⁴⁵ which do not decide upon the actual symmetry, agree with our findings in the sense that they also exclude the C_{2v} symmetry. This is useful in giving up any doubts about a possible accidental degeneracy. The C_{3v} symmetry derived in this paper agrees with the result from uniaxial stress measurements.³⁸

The observed BT 39 together with our observation that one cannot create a nonrandom distribution of the SH^- impurities with $[110]$ -polarized uv light, indicates that SH^- in KCl is reorienting among eight equivalent potential wells along $\langle 111 \rangle$, while it performs its own vibrational stretching mode.

V. DISCUSSION

A. Anisotropy of the molecular ion

The expressions (5) and (6) show that the s/q ratio for C_{3v} and the r/q ratio for the C_{4v} point group are directly

related to the anisotropy of the free molecular ion, i.e., the ratio a_3/a . For C_{2v} this correspondence is not present, since the orthorhombic symmetry introduces a third independent component in the Raman tensor.

For CN^- in KCl and KBr the small s/q ratio reflects the small difference between the derived polarizabilities parallel (a_3) and perpendicular (a) to the molecular axis. In the limit of zero anisotropy the A_1 mode of C_{4v} is detected as a $T:A$ mode.¹² Small anisotropy of the derived polarizability tensor of the stretching mode may yield the observation of a higher symmetry than the actual defect symmetry: It is a typical case of accidental degeneracy, one of the major restrictions intrinsic to the BT method.

The ratio a_3/a is calculated for the Raman tensors (5a) and (5b) from the experimental s/q and r/q ratios in Table II. The two possible solutions of the quadratic equation are presented in Fig. 4. We favor the upper branch of the solutions as the physical one, since the change of sign of a_3/a for the isoelectronic impurities OH^- and SH^- in the same host lattice does not seem realistic. Moreover, one can argue, following Peascoe and Klein,⁸ that in OH^- and SH^- mainly the bonding σ electrons will be influenced by the stretching vibration, in contrast with the nonbonding π electrons. Therefore, a ratio a_3/a larger than unity is more likely. It is also interesting to note the different behavior of the molecular (ion) polarizability and its derivative to the stretching mode: In Fig. 4 it is shown that the anisotropy of the derived polarizability is small for CN^- and larger for OH^- , a situation which is apparently reversed for the polarizability itself.^{26,34}

The s/q and r/q ratios of O_2^- do not permit an interpretation in terms of $x'x'/z'z'$ and $y'y'/z'z'$ of (5c) and (6c). The set of coupled quadratic equations yields four solutions for the ratios $x'x'/z'z'$ and $y'y'/z'z'$ with different magnitudes and signs. Elimination of one of these solutions is not obvious, since it is difficult to estimate the influence of the A_1 mode on the bonding π electrons.

The r/q ratio of approximately 1 for the O_2^- vibration in NaCl suggests a trial solution of the coupled quadratic equations of $z'z'/x'x' \approx z'z'/y'y' \approx 1$. However, these tri-

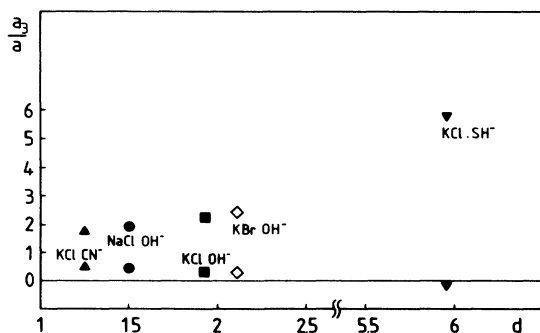


FIG. 4. Representation of the molecular anisotropy a_3/a for defects with C_{3v} and C_{4v} symmetry as a function of the difference d between the two solutions for a_3/a of the quadratic equation with parameters s/q and r/q (see Table II).

al values are not at all compatible with the s/q ratio of 0.40. For O_2^- in NaCl the accidental degeneracy, i.e., the observation of the D_{3d} point group for a defect with D_{2h} symmetry, is clearly not related to the small anisotropy of the derived polarizability.

B. Coupling of the stretching vibration to the tunneling motion

Tunneling sidebands of the stretching mode, originating from Raman transitions between the ground-state tunneling multiplet and the one in the excited vibrational state, possess polarization properties different from those of the stretching peak. When not completely resolved, these sidebands contribute to either the A_{1g} , the T_{2g} , or the E_g spectra of the stretching mode, which quantitatively influences the s/q and r/q ratios.

Both the intensity and the splitting of the tunneling sidebands are larger for a larger overlap between the wave functions of different rotational states in the ground and the excited vibrational state.⁹ This yields the fortunate situation that for systems with poorly resolved tunneling sidebands, the influence of the latter on the s/q and r/q ratios is comparatively small.

For the CN^- defect in KCl (tunneling splitting 1.2 cm^{-1}) Durand and Lüty¹¹ have detected sidebands of the stretching mode permitting the determination of the C_{3v} symmetry of the equilibrium orientations of CN^- . With a less powerful laser and samples with a relatively high CN^- concentration—which washes out the sideband fine structure—we obtained evidence for these tunneling sidebands, albeit only in the T_{2g} spectrum. This is demonstrated by comparing the integrated areas of the polarized Raman intensities of several measurements, yielding an s/q value of 0.057 ± 0.008 , which was systematically larger than the one derived from the peak heights (0.036 ± 0.007). In contrast, the r/q values are equal within experimental error for both ways of calculation. The expressions (8) illustrate the different behavior of these two IP ratios: The s/q value displays the T_{2g} tunneling sidebands of the stretching mode in the integrated spectrum. We deduce a sideband intensity in the yz spectrum to be 1% of the yy intensity of the stretching peak in agreement with the earlier results.¹¹ No such effect was observed for O_2^- in different host lattices, in agreement with the much smaller tunneling splitting ($\approx 10^{-6} \text{ cm}^{-1}$) of this center.

C. Interaction with the host lattice

Table II shows that in KCl and KBr the s/q and r/q values of the stretching modes of O_2^- and OH^- are rather similar. However, in NaCl the smaller lattice parameter yields quantitatively different polarized Raman intensities.

1. NaCl: O_2^-

For the O_2^- ion EPR measurements^{35–37} established a different electronic structure depending on the alkali halide host. The molecular axis is oriented along $\langle 110 \rangle$ in every crystal. However, in potassium and rubidium halides the probability density of the wave function of the

unpaired $p\pi$ electron is the highest in a $\{001\}$ plane containing the molecular axis, but in sodium halides this density is maximum in a $\{110\}$ plane. Moreover, in KCl and KBr a covalent bond exists between these $p\pi$ orbitals and the nearest alkali atoms, which is not the case in NaCl.³⁷ Possibly, the different electronic structure of O_2^- in NaCl is reflected in the Raman spectra of its stretching mode, yielding the surprising result of an observed D_{3d} symmetry.

2. NaCl:OH⁻

Considering the C_{4v} point group for the NaCl:OH⁻ system, it should be emphasized that the value of 0.06 for s/q cannot originate from tunneling sidebands [see (8)], since the only Raman-allowed sideband intensities for this symmetry appear in the E_g spectrum. Therefore, the measured IP correspond to an observed BT 60, associated with either the A_g mode of the $D_{2h}[110]$ symmetry, or the A' mode of the C_{1h} symmetry, reflecting a tilting of the OH⁻ axis away from $[100]$ into two equivalent $\{011\}$ or $\{001\}$ planes. This small tilting angle agrees with the results of Baur and Salzman,^{46,47} who calculated the $\langle 100 \rangle$ orientation of the OH⁻ axis not to be the lowest-energy configuration: The potential energy decreases for a small deviation from the $\langle 100 \rangle$ direction towards the next-nearest-neighbor Cl⁻ ion.

VI. CONCLUSION

The BT analysis of the polarized Raman spectra of the stretching mode is demonstrated to be a new and dependable method to derive the equilibrium orientations of static or reorienting substitutional diatomic molecular ions in cubic crystals. It is stressed once more that the Raman tensor of the totally symmetric stretching mode *does* reflect the symmetry of the defect. This has not been appreciated up until the present investigation.⁴⁸ Consequently, the information retrievable from the polarized Raman data of the stretching mode is considerably larger than traditionally and implicitly accepted.

The experimental results, confirmed by earlier work and different techniques, underline the general dependability of the method. Its main advantages are (i) simplicity of the experimental technique, i.e., no secondary field is needed, and (ii) the possibility of measurements on strong signals, i.e., on the stretching mode itself and not on the weak tunneling sidebands. The latter point implies the applicability to centers with unresolvably small tunneling splittings, such as O_2^- . Application to defects, which are not paramagnetic, is also possible, making the

Raman scattering technique in a sense complementary to EPR.

In general, it should be mentioned that the BT of the stretching mode of a reorienting molecular system is expected to be temperature dependent. However, at temperatures corresponding to thermal energies below the height of the multiwell potential barriers, the Raman process probes the stretching motion within one orientational potential well.

It could be interesting to investigate the OH⁻ defect in KI, in which the molecular axis is oriented along $\langle 110 \rangle$.^{27,28,49,50} A comparison of the anisotropy of the derived polarizability between OH⁻ oriented along $\langle 100 \rangle$ and $\langle 110 \rangle$ can give information about the influence of the host lattice on its molecular properties. We are planning additional measurements on O_2^- in other alkali halide host lattices in order to obtain more detailed information about the vibronic coupling of this center.

The present study is relevant in the context of the so-called F_H centers, in which the molecular impurity is adjacent to an F center in a next-nearest-neighbor position. For these defects electron-nuclear double-resonance (ENDOR) measurements on the F center have probed the orientation of the molecular ion.⁵¹ It would be interesting to compare the ENDOR data to the Raman data of both the isolated molecular impurity and its associated F_H center. The $F_H(CN^-)$ centers are of considerable actual interest because of their vibrational luminescence under F -band excitation,^{52,53} offering perspectives for the design of infrared lasers.⁵⁴ The Raman technique, together with the behavior-type method, is certainly a suitable approach to study the coupling between electronic and vibrational states in these systems.

ACKNOWLEDGMENTS

This work was supported by the IIKW (Interuniversitair Instituut voor Kernwetenschappen), the NFWO (Nationaal Fonds voor Wetenschappelijk Onderzoek), and the Geconcerteerde Acties (Ministerie van Wetenschapsbeleid) to which the authors are greatly indebted. We wish to thank D. Schmid for kindly providing us with the O_2^- -doped samples and F. Lüty for critically reading the manuscript and supplying some KCl:CN⁻ samples. We also thank R. van de Walle for performing preliminary measurements and A. Bouwen for excellent experimental support. Two of us (H.F. and W.J.) were supported by NFWO (National Fund for Scientific Research), Belgium.

¹A. F. Devonshire, Proc. R. Soc. London, Ser. A **153**, 601 (1936).

²H. B. Shore, Phys. Rev. **151**, 570 (1966).

³M. Gomez, S. P. Bowen, and J. A. Krumhansl, Phys. Rev. **153**, 1009 (1967).

⁴V. Narayanamurti and R. O. Pohl, Rev. Mod. Phys. **42**, 201 (1970).

⁵F. Bridges, in *Paraelectric Phenomena*, Vol. 5 of *Chemical Rubber Company Critical Reviews* (Chemical Rubber Co., Cleveland, 1975).

⁶W. R. Fenner and M. V. Klein, in *Light Scattering Spectra in Solids*, edited by G. Wright (Springer, New York, 1969).

⁷R. Callender and P. S. Pershan, Phys. Rev. A **2**, 672 (1970).

⁸J. G. Peascoe and M. V. Klein, J. Chem. Phys. **59**, 2394 (1973).

- ⁹J. G. Peascoe, W. R. Fenner, and M. V. Klein, *J. Chem. Phys.* **60**, 4208 (1974).
- ¹⁰W. Holzer, W. F. Murphy, and H. J. Bernstein, *J. Mol. Spectrosc.* **32**, 13 (1969).
- ¹¹D. Durand and F. Lüty, *Phys. Status Solidi B* **81**, 443 (1977).
- ¹²J. F. Zhou, E. Goovaerts, and D. Schoemaker, *Phys. Rev. B* **29**, 5509 (1984).
- ¹³E. Goovaerts, J. F. Zhou, W. Joosen, and D. Schoemaker, *Cryst. Lattice Defects Amorph. Mater.* **12**, 317 (1985).
- ¹⁴J. F. Zhou, E. Goovaerts, and D. Schoemaker, *Phys. Rev. B* **29**, 5533 (1984).
- ¹⁵W. Joosen, J. F. Zhou, E. Goovaerts, and D. Schoemaker, *Phys. Rev. B* **31**, 6709 (1985).
- ¹⁶W. Joosen, E. Goovaerts, and D. Schoemaker, *J. Lumin.* **31-32**, 317 (1984).
- ¹⁷W. Joosen, E. Goovaerts, and D. Schoemaker, *Phys. Rev. B* **32**, 6748 (1985).
- ¹⁸W. Joosen, C. Sierens, and D. Schoemaker, *Solid State Commun.* **63**, 69 (1987).
- ¹⁹M. Leblans, W. Joosen, E. Goovaerts, and D. Schoemaker, *Phys. Rev. B* **35**, 2405 (1987).
- ²⁰M. Leblans, W. Joosen, D. Schoemaker, A. Mabud, and F. Lüty (unpublished).
- ²¹W. Joosen, E. Goovaerts, and D. Schoemaker, *Phys. Rev. B* **35**, 8215 (1987).
- ²²W. Joosen, E. Goovaerts, and D. Schoemaker, *Phys. Rev. B* **34**, 1273 (1986).
- ²³M. Vanhimbeeck, H. De Raedt, W. Joosen, and D. Schoemaker, *Europhys. Lett.* **4**, 141 (1987).
- ²⁴H. Härtel, *Phys. Status Solidi* **42**, 369 (1970).
- ²⁵R. D. Kirby, A. E. Hughes, and A. J. Sievers, *Phys. Rev. B* **2**, 481 (1970).
- ²⁶G. Zibold and F. Lüty, *J. Nonmetals* **1**, 1 (1972).
- ²⁷W. Heinicke and F. Lüty, *Bull. Am. Phys. Soc.* **17**, 143 (1972).
- ²⁸S. Kapphan and F. Lüty, *J. Phys. Chem. Solids* **34**, 969 (1973).
- ²⁹F. Lüty, *Phys. Rev. B* **10**, 3667 (1974).
- ³⁰W. D. Seward and V. Narayanamurti, *Phys. Rev.* **148**, 463 (1966).
- ³¹R. L. Pompei and V. Narayanamurti, *Solid State Commun.* **6**, 645 (1968).
- ³²F. Lüty, *Phys. Rev. B* **10**, 3677 (1974).
- ³³H. U. Beyeler, *Phys. Rev. B* **11**, 3078 (1975).
- ³⁴A. Diaz-Gongora and F. Lüty, *Phys. Status Solidi B* **86**, 127 (1978).
- ³⁵W. Känzig and M. H. Cohen, *Phys. Rev. Lett.* **3**, 509 (1959).
- ³⁶W. Känzig, *J. Phys. Chem. Solids* **23**, 479 (1962).
- ³⁷H. R. Zeller and W. Känzig, *Helv. Phys. Acta* **40**, 845 (1967).
- ³⁸W. Kuch and U. Dürr, *J. Phys. Chem. Solids* **42**, 677 (1981).
- ³⁹L. N. Ovander, *Opt. Spektrosk.* **9**, 571 (1960) [*Opt. Spectrosc. (USSR)* **9**, 302 (1960)].
- ⁴⁰R. M. Martin and L. M. Falicov, in *Light Scattering in Solids*, edited by M. Cardona (Springer-Verlag, Berlin, 1975), pp. 83–88.
- ⁴¹The s/q ratio, defined for dynamical modes of defects in cubic lattices, directly corresponds to the depolarization ratio ρ of vibrations in liquids. However, in the liquid phase, the IP q , r , and s are no longer independent and the relation $q - r = 2s$ holds. This results from the *continuous* spatial average over the possible orientations of the molecule in contrast with the *discrete* average in the cubic crystal lattice. [See W. Hayes and R. Loudon, *Scattering of Light by Crystals* (Wiley, New York, 1977), pp. 46–47].
- ⁴²D. A. Long, *Raman Spectroscopy* (McGraw-Hill, New York, 1977), pp. 46–47.
- ⁴³C. K. Chi and E. R. Nixon, *J. Phys. Chem. Solids* **33**, 2101 (1972).
- ⁴⁴W. E. Bron and R. W. Dreyfus, *Phys. Rev. Lett.* **16**, 165 (1966).
- ⁴⁵J. Otto, *Phys. Status Solidi B* **142**, 105 (1987).
- ⁴⁶M. E. Baur and W. R. Salzman, *Phys. Rev.* **151**, 710 (1966).
- ⁴⁷M. E. Baur and W. R. Salzman, *Phys. Rev. Lett.* **18**, 590 (1967).
- ⁴⁸H. U. Beyeler, *Phys. Rev. B* **10**, 2614 (1974).
- ⁴⁹W. M. Kelly and F. Bridges, *Solid State Commun.* **20**, 119 (1976).
- ⁵⁰W. M. Kelly and F. Bridges, *Phys. Rev. B* **18**, 4606 (1978).
- ⁵¹J. M. Spaeth (private communication).
- ⁵²Y. Yang and F. Lüty, *Phys. Rev. Lett.* **51**, 419 (1983).
- ⁵³Y. Yang, W. von der Osten, and F. Lüty, *Phys. Rev. B* **32**, 2724 (1985).
- ⁵⁴W. Gellermann, Y. Yang, and F. Lüty, *Opt. Commun.* **57**, 196 (1986).